Advances in Pharmacological and Pharmaceutical Sciences

WILEY

RESEARCH ARTICLE OPEN ACCESS

Accelerated Wound Healing Using Biocellulose Dressings Enriched With *Laportea decumana* Extract in Polymicrobial Infection Wound Models

Yulia Yusrini Djabir[1] | Dwi Novrianty Busaeri[1] | Muhammad Haryandi[1] | Nurhasni Hasan[1] | Habibie Habibie[1] | Djulfikri Mewar[2] | Hien Minh Nguyen[3] | Aryadi Arsyad[4]

[1]Faculty of Pharmacy, Hasanuddin University, Makassar, Indonesia | [2]Department of Pharmacy, Institute of Health Science Maluku Husada, Maluku, Indonesia | [3]Research Group in Pharmaceutical and Biomedical Sciences, Faculty of Pharmacy, Ton Duc Thang University, Ho Chi Minh City, Vietnam | [4]Faculty of Medicine, Hasanuddin University, Makassar, Indonesia

Correspondence: Yulia Yusrini Djabir (yulia.yusrini@unhas.ac.id)

Received: 26 August 2025 | **Revised:** 19 February 2026 | **Accepted:** 25 February 2026

Academic Editor: Anjali Chauhan

Keywords: biocellulose dressing | cell proliferation | *Laportea decumana* | maturation | wound healing

ABSTRACT

Laportea decumana (Roxb.) Wedd. is known for its analgesic, antioxidant, anti-inflammatory, and antibacterial properties. This study aimed to evaluate the wound-healing effects of LDE incorporated into a biocellulose dressing for the treatment of polymicrobial-infected wounds. The metabolite profile of LDE was characterized using UPLC-Q-TOF/MS. Biocellulose dressings were prepared with and without 4% LDE for the *in vivo* study. Fifteen male rats were each subjected to three biopsy punch wounds, which were infected with a polymicrobial mix of *Staphylococcus aureus*, *Staphylococcus epidermidis*, and *Pseudomonas aeruginosa*. The wounds were treated with either blank or 4% LDE-fortified biocellulose dressing, or left untreated for 14 days. Wound diameters were measured daily, and histological analyses were conducted on Days 3, 7, and 11 to evaluate the inflammatory, proliferative, and maturation phases of wound healing. *In vivo* experiments showed that wounds treated with 4% LDE-fortified biocellulose had significantly smaller diameters from Day 11 onward compared to untreated wounds or blank control. While all wounds exhibited edema and leukocyte infiltration during the inflammatory phase, treatment with 4% LDE significantly enhanced granulation tissue formation, fibroblast activity, and collagen deposition in the proliferative phase. During maturation, LDE-fortified dressings accelerated re-epithelialization. In conclusion, the 4% LDE-fortified biocellulose dressing exhibited wound-healing effects in a rat model of infected wounds by promoting cell proliferation and accelerating the maturation phase of wound repair. Further studies are needed to clarify the underlying antimicrobial and inflammatory mechanisms.

1 | Introduction

Acute and chronic wounds represent a major global public health burden. In particular, chronic wounds complicated by polymicrobial infections contribute substantially to morbidity and mortality worldwide [1]. Under physiological conditions, wound repair proceeds through a tightly regulated sequence of overlapping inflammatory, proliferative, and remodeling phases [2]. However, in the presence of infection, this tightly regulated process is disrupted, leading to significantly prolonged healing times that, in some cases, can extend for years. Severe infections may further progress to complications such as gangrene, often requiring surgical interventions, including amputation [3]. Moreover, the increasing prevalence of antibiotic-resistant pathogens presents a challenge in managing polymicrobial wound infections, emphasizing the need for alternative

This is an open access article under the terms of the Creative Commons Attribution License, which permits use, distribution and reproduction in any medium, provided the original work is properly cited.

Copyright © 2026 Yulia Yusrini Djabir et al. *Advances in Pharmacological and Pharmaceutical Sciences* published by John Wiley & Sons Ltd.

therapeutic approaches that can help control infections while reducing reliance on conventional antibiotics.

A promising strategy for managing wound infections involves using wound dressings that provide a protective barrier against microbial invasion. Among these, biocellulose-based dressings have gained considerable attention due to their distinctive physicochemical properties. Bacterial cellulose, naturally synthesized by acetic acid bacteria, particularly from the *Acetobacter* genus, serves as a versatile biomaterial for wound care applications. Its structural properties can be tailored by modifying the culture conditions, allowing for enhanced functionality in biomedical applications [4]. Its unique properties, including moldability, flexibility, scalable production, and excellent biocompatibility, make bacterial biocellulose a highly promising material for wound dressings [5]. Furthermore, its nanoporous structure and high liquid absorption capacity make it well-suited for wound healing by maintaining a moist environment, facilitating oxygen exchange, and supporting tissue regeneration [6]. However, in addition to the structural properties of wound dressings, effective management of polymicrobial-infected wounds also requires the incorporation of bioactive compounds with potent antibacterial, anti-inflammatory, and wound-healing activities.

Laportea decumana (Roxb) Wedd, a member of the Urticaceae family, is a medicinal plant traditionally utilized by indigenous communities in Papua and Maluku Islands in Indonesia for wound treatment; however, its therapeutic potential remains underexplored. Phytochemical analyses of *L. decumana* have revealed its antibacterial efficacy against *Staphylococcus aureus*, as well as its antioxidant and cytotoxic activities against breast cancer cells, indicating its potential as a multifunctional therapeutic agent [7]. Additional studies have demonstrated the ability of *L. decumana* leaf compounds to inhibit cyclooxygenase-2 (COX-2), thereby exerting anti-inflammatory effects and scavenging free radicals [8]. In line with these findings, a previous study confirmed the analgesic and anti-inflammatory properties of topically applied *L. decumana* leaf extract in a rat model, with its mechanism involving the inhibition of interleukin-6 (IL-6) release at inflamed sites [9].

Despite its diverse bioactivities, the wound-healing efficacy of *L. decumana* has not been investigated in polymicrobial-infected wounds. Moreover, existing studies are largely limited to extract-based assays or conventional formulations that are inadequate for sustained local delivery or effective modulation of the wound microenvironment. Recent studies have demonstrated the benefits of integrating plant-derived phytochemicals into advanced biomaterial-based wound dressings to enhance wound healing and antimicrobial efficacy [10, 11]. In recent years, various plant-derived bioactives, such as those from *Aloe vera* or *Centella asiatica*, have been successfully incorporated into advanced biomaterial-based dressings to enhance antimicrobial activity, fibroblast compatibility, and tissue regeneration [12]. However, to the best of our knowledge, *L. decumana* has not previously been integrated into a structured biomaterial delivery platform.

Therefore, this study aimed to evaluate the wound-healing efficacy of *L. decumana* leaf extract formulated in biocellulose dressing using a polymicrobial-infected rat wound model. This study introduces a novel approach by integrating *L. decumana*–derived bioactive compounds with the structural and functional advantages of biocellulose to enhance the healing process in complex wound infections.

2 | Materials and Methods

2.1 | Sample Collection and Extraction

The leaves of *Laportea decumana* were collected from Wakal Village, Leihitu District, Central Maluku Regency, Ambon City (Figure 1). The plant was taxonomically identified by a pharmacognosist at the Laboratory of Pharmacognosy, Hasanuddin University, and documented under reference number 037/SKIT/Farmakognosi/IX/2024. A total of 500 g of dried *L. decumana* leaf powder was macerated in 70% EtOH at room temperature for 72 h. The mixture was filtered, and the remaining plant residue was subjected to repeated maceration until the solvent appeared colorless, ensuring exhaustive extraction of the phytochemicals. The combined filtrates were concentrated under reduced pressure using a rotary evaporator at a controlled temperature to yield a thick EtOH extract of *L. decumana* leaves.

2.2 | Phytochemical Profiling by Ultra-Performance Liquid Chromatography System Coupled to a Quadrupole Time-of-Flight Mass Spectrometer (UPLC-Q-TOF/MS)

The separation was achieved using an Agilent RRHD Eclipse XDB-C18 column (80 Å, 2.1 × 100 mm, 1.8 μm) (p/n: 981758-902) on the Agilent 1290 Infinity II LC system. The mobile phase consisted of water and acetonitrile for negative-mode data acquisition. The gradient elution program was as follows: 0 min: 5% B; 0.5 min: 20% B; 50 min: 95% B (held for 15 min). After elution, a 5-min equilibration step was used to prepare the column for the next injection. The total run time was 70 min per sample. The system operated in constant flow mode, with a flow rate of 0.3 mL/min. 5 μL of the sample was injected into the system. The autosampler and column compartment temperatures were set at 10°C and 30°C, respectively.

The Q-TOF mass spectrometer was operated in negative ionization mode using a dual Agilent Jetstream source with the following settings: sheath gas flow of 11 L/min at 400°C, capillary voltage at +3.5 kV (positive) and −3.5 kV (negative), nebulizer pressure at 35 psi, and drying gas flow of 5 L/min at 300°C. Three levels of collision energy (0, 20, and 40 V) were used to capture metabolites over a mass range of *m/z* 50 to 1200 using the all-ion MS/MS scan mode. The reference masses used for data acquisition were m/z 112.9855 and 1033.9881 in negative mode. The scan rate was set to 3 spectra/s. Chemical structures were identified by combining UPLC-Q-TOF/MS data with the Agilent METLIN Personal Metabolite Database.

2.3 | Biocellulose Preparation

The preparation of biocellulose was performed as described in a study conducted by Hasan et al. using *Acetobacter intermedius* BC-4 (Department of Manufacturing Pharmacy, Pusan National University, Korea) [13]. The bacteria were cultivated in culture media supplemented with 2% glucose, 0.5% yeast extract, 0.5% Bacto peptone, citric acid, and $Na_2HPO_4 \cdot 12\,H_2O$, for 15 days at a pH of 6. Biocellulose pellicles started to form after 7 days, and when the suitable thickness was achieved, the pellicles were



FIGURE 1 | The plant of *Laportea decumana*.

collected by deionized water immersion (90°C for 2 h). The biocellulose pellicles were then submerged in a 0.5 M sodium hydroxide (NaOH) solution and boiled for 20 min, followed by multiple rinses with deionized water. The pellicles were then submerged in a 1% NaOH solution for 2 days to achieve a neutral pH and subsequently freeze-dried. Once dried, the pellicles were stored at a temperature of ±25°C for future use.

Biocellulose dressings were loaded with 4% (w/v) *L. decumana* extract (LDE) using an immersion adsorption method. The concentration was selected based on a prior report demonstrating biological activity of the crude extract at this level in topical applications [14]. Briefly, sterile biocellulose sheets were submerged in the extract solution and incubated for 24 h at room temperature to allow passive diffusion and incorporation of bioactive compounds into the nanofibrillar matrix. After incubation, the dressings were removed and gently blotted to eliminate excess surface solution prior to *in vivo* application.

2.4 | Polymicrobial Preparation

The polymicrobial strains used to model infected wounds included *Staphylococcus aureus ATCC 25923, Staphylococcus epidermidis ATCC 12228,* and *Pseudomonas aeruginosa ATCC 27853*, which were obtained from the Laboratory of Microbiology, Hasanuddin University, Indonesia. These strains were selected due to their frequent involvement in clinical wound infections, where *S. aureus* is a primary pathogenic species, *S. epidermidis* represents a common skin commensal associated with biofilm formation, and *P. aeruginosa* is a predominant Gram-negative pathogen in chronic and polymicrobial wounds. The bacterial cultures were rejuvenated in Nutrient Agar (Merck, Germany) and incubated at 37°C for 24 h, then prepared in suspension in physiological sodium chloride (0.9% NaCl) solution, and the concentration was adjusted to match a 0.5 McFarland standard.

2.5 | Animal Preparation

Eighteen male Wistar rats, aged 2–3 months, and weighing 150–250 g, were obtained from the Laboratory of Pharmacology and Toxicology, Hasanuddin University, Indonesia. Prior to experimentation, the animals were acclimatized to laboratory conditions for 1 week to minimize stress and ensure environmental adaptation. Throughout the study, all rats were maintained under standard housing conditions, which included regulated temperature and humidity, as well as a 12-h light/dark cycle.

2.6 | Experimental Protocols

The rats were anesthetized using ether via inhalation due to its rapid induction and short procedural duration; all animals were exposed under identical conditions to minimize variability in stress or inflammatory responses. The dorsal area of each rat was shaved, dividing it into two sections: the left and right sides of the back. Each rat received three circular full-thickness excisional wounds (6 mm in diameter) on the dorsal surface using a sterile biopsy punch. The wounds on each animal were designated as A, B, and C, and each wound was assigned to a different treatment group: untreated control, blank biocellulose dressing, or biocellulose dressing containing LDE. This within-animal design was employed to minimize interanimal variability.

Each wound was inoculated with 50 μL of a polymicrobial bacterial suspension at a concentration of 1×10^7 CFU/mL. The bacterial concentration was selected based on a previous study using a skin and wound co-culture model [15], which demonstrated that this inoculum level reliably establishes polymicrobial infection and biofilm formation without excessive cytotoxicity. The wounds were subsequently sealed with a polyurethane film dressing (Tegaderm Transparent Dressing; 3M Health Care, St. Paul, MN) and left untouched for 24 h before applying the assigned treatment for each wound.

Treatments were applied once daily for 14 consecutive days. Wound morphology and diameter were measured daily using a Vernier caliper. The measurements of the wound diameters were done in four dimensions (vertical, horizontal, left, and right diagonals). The rate of wound healing (R) was calculated according to the following formula:

$$R = \left[\frac{(D_n - D_0)}{D_n}\right] \times 100 \quad (1)$$

where R = the rate of wound healing, D_n = wound diameter on Day n, and D_0 = wound diameter on Day 0.

Rats were euthanized at predetermined time points to represent different phases of wound healing: Day 3 (inflammatory phase, $n = 5$ rats), Day 7 (proliferative phase, $n = 5$ rats), and Day 11 (early maturation phase, $n = 5$ rats). The remaining animals ($n = 3$ rats) were maintained until complete wound closure to evaluate the overall healing duration. The experimental protocol is depicted in Figure 2.

2.7 | Histopathological Analysis

Wound tissues were excised from the dorsal area, measuring approximately 20 × 20 mm and extending to the fascia, including 5 mm of healthy tissue surrounding the wound. The collected specimens were then fixed in 10% formalin for 48 h. Wound specimens were processed using a tissue processor (Thermo Fisher, USA) and prepared into histological slides, following the method described by Busaeri et al. (2025) [14]. After being stained with hematoxylin and eosin (HE), the tissue sections were seen under a light microscope at 100x and 200x magnifications. Histopathological evaluation was performed using

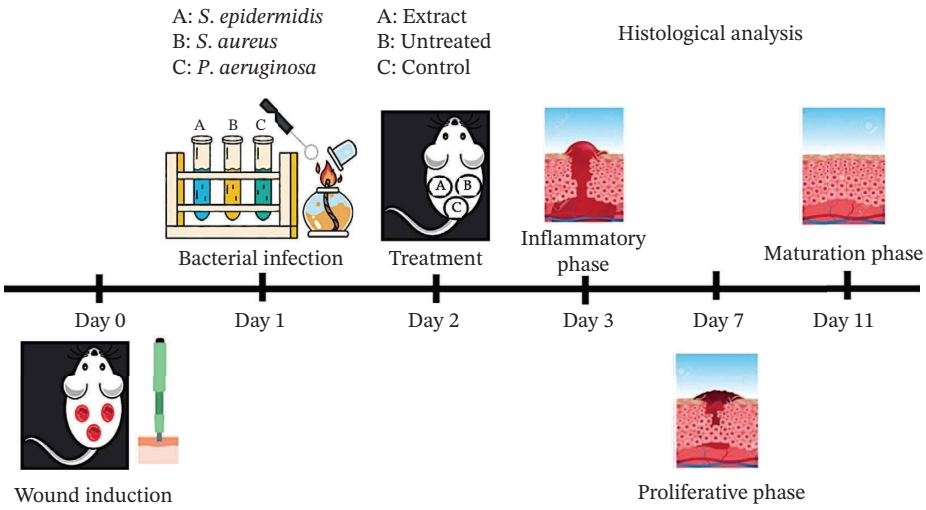


FIGURE 2 | The scheme of experimental protocols.

predefined morphological criteria, including inflammatory cell infiltration, fibroblast proliferation, granulation tissue formation, and re-epithelialization, to allow consistent comparison among treatment groups.

2.8 | Statistical Analysis

All data were analyzed using SPSS software. For each time point, wound diameter and wound-healing percentage values represent group means calculated from measurements obtained from individual animals, and variability is expressed as standard deviation (SD). Data normality was assessed prior to statistical testing. Normally distributed data were analyzed using one-way ANOVA, followed by Tukey's HSD post hoc test when significant differences were detected ($p < 0.05$). For data that did not meet normality assumptions, the Kruskal–Wallis test was applied. A p value < 0.05 was considered statistically significant.

3 | Results

3.1 | Yield of *L. decumana* Leaf Extract

Maceration of 500 g of dried *Laportea decumana* leaf powder produced 57 g of concentrated extract, corresponding to a yield of 11.4%.

3.2 | Phytochemical Analysis of *L. decumana* EtOH Extract

The components identified in the *L. decumana* EtOH extract using a UPLC-Q-TOF/MS in negative ionization mode are presented in Table 1. The Q-TOF-MS provides accurate precursor and product ion information with a mass error of less than 5 ppm, ensuring high precision in the identification and characterization of compounds. The compounds were identified based on retention time, Agilent METLIN personal metabolite library information, and MS databases. The chromatogram of the EtOH *L. decumana* leaf extract is depicted in Figure 3.

The UPLC-Q-TOF/MS analysis in negative ion mode identified **42** distinct compounds in the EtOH extract, classified into several chemical groups, with glycosides as the most abundant, followed by alkaloids, steroids, triterpenoids, sesquiterpenes, flavonoids, and other compounds. The detected glycosides included rebaudioside B **(1)**, corchoionoside B **(2)**, lyciumoside IV **(7)**, ptelatoside A **(11)**, oleaside E **(12)**, cimicifugoside **(30)**, and glucosyl (2E,6E,10x)-10,11-dihydroxy-2,6-farnesadienoate **(16)**. Among the alkaloids, palmatine **(10)**, triphyllin B **(13)**, integerrenine **(14)**, daphnoline **(18)**, zizyphine A **(19)**, mucronine B **(20)**, adlupone **(22)**, 2′-norberbamunine **(28)**, and haplophytine **(35)** were identified. Steroid-related compounds detected included sitosteryl ester **(29)**, ergosterol acetate **(34)**, stigmasteryl ester **(38)**, stigmastan-3,5-diene **(39)**, conicasterol B **(40)**, and stellasterol **(42)**. The triterpenoids comprised theasapogenol A **(21)**, salannin **(26)**, and 24-norursa-3,12-diene **(37)**, while sesquiterpenes included artesunate **(9)**, 11α-acetoxykhivorin **(15)**, oleandolide **(25)**, and thapsigargin **(33)**. The identified flavonoids were 3-hydroxy lidocaine glucuronide **(6)**, capparilloside A **(8)**, and toonacilin **(27)**. Additionally, several other compounds were detected, including 3-O-trans-feruloyleuscaphic acid **(24)** from the phenolic group, 3-(2,5-dimethoxyphenyl)propanoic acid **(3),** and 4-methoxycinnamic acid **(5)** from the carboxylic and cinnamic acid group; hydroxyphthioceranic acid (C43) **(31)** and linoleic acid **(32)** from the fatty acid group; 1,3,8-trihydroxy-4-methyl-2,7-diprenylxanthone **(36)** from the xanthone group; and erythrinasinate A **(41)** from the coumaric acid group.

3.3 | Effect of *L. decumana* Biocellulose Dressing on Wound Size and Appearance

Over the 14-day observation period, wound diameter decreased progressively in all treatment groups from an initial size of 6 mm. This reduction was observed in untreated wounds as well as in wounds treated with biocellulose alone or biocellulose combined with LDE. During the early phase (Days 1–7), no statistically significant differences in wound diameter were detected among groups. On Day 3, wound diameters were 5.97 ± 0.09 mm (untreated), 5.06 ± 0.76 mm (blank biocellulose), and 5.97 ± 0.09 mm (biocellulose + LDE). Morphological evaluation at this time point revealed the presence of pus and exudate in all wounds (Figure 4).

By Day 7, wounds treated with biocellulose plus LDE exhibited a trend toward smaller wound diameter (4.41 ± 0.82 mm) and reduced exudate compared with wounds treated with

TABLE 1 | Chemical compositions of the *L. decumana* EtOH extract analyzed by UPLC-Q-TOF/MS (negative mode).

No.	RT	Exp. mass *m/z*	Calc. mass *m/z*	Type	Formula	Tentatively identified compounds	Diff (ppm)	Peak area
1	11.22	804.378	804.378	Glycoside	$C_{38}H_{60}O_{18}$	Rebaudioside B	0.09	31,285,062
2	11.656	400.1733	400.1733	Glycoside	$C_{19}H_{28}O_9$	Corchoionoside B	0.02	18,579,439
3	13.156	210.0891	210.0892	Carboxylic acid	$C_{11}H_{14}O_4$	3-(2,5-Dimethoxyphenyl)propanoic acid	−0.72	3,551,074
4	13.853	188.105	188.1049	Carboxylic acid	$C_9H_{16}O_4$	Nonic acid	0.49	26,727,807
5	14.324	178.0627	178.063	Cinnamic acid	$C_{10}H_{10}O_3$	4-Methoxycinnamic acid	−1.58	2,151,151
6	16.482	426.2018	426.2002	Flavonoid	$C_{20}H_{30}N_2O_8$	3-Hydroxy lidocaine glucuronide	3.65	2,492,354
7	17.656	776.4192	776.4194	Glycoside	$C_{38}H_{64}O_{16}$	Lyciumoside IV	−0.35	31,013,184
8	19.034	334.1162	334.1165	Flavonoid	$C_{16}H_{18}N_2O_6$	Capparilloside A	−1	1,844,677
9	20.935	384.1783	384.1784	Sesquiterpene	$C_{19}H_{28}O_8$	Artesunate	−0.35	28,286,305
10	22.034	352.1552	352.1548	Alkaloid	$C_{21}H_{22}NO_4$	Palmatine	1.01	1,743,752
11	24.912	414.154	414.1526	Glycoside	$C_{19}H_{26}O_{10}$	Ptelatoside A	3.29	3,891,565
12	24.947	840.4138	840.4144	Glycoside	$C_{42}H_{64}O_{17}$	Oleaside E	−0.71	2,246,718
13	27.092	642.2182	642.216	Alkaloid	$C_{29}H_{38}O_{16}$	Triphyllin B	3.51	4,200,892
14	27.598	534.3193	534.3206	Alkaloid	$C_{31}H_{42}N_4O_4$	Integerrenine	−2.52	40,085,924
15	28.8	644.2843	644.2833	Sesquiterpene	$C_{34}H_{44}O_{12}$	11α-Acetoxykhivorin	1.54	1,196,912
16	31.539	432.2343	432.236	Glycoside	$C_{21}H_{36}O_9$	Glucosyl (2E,6E,10x)-10,11-dihydroxy-2,6-farnesadienoate	−3.89	2,191,237
17	32.447	496.1969	496.1945	Glycoside	$C_{24}H_{32}O_{11}$	(7R∗,8R∗)-3-Methoxy-3′,4,7,9,9′-pentahydroxy-8,4′-oxyneolignan 4-xyloside	4.85	12,036,862
18	32.761	580.2578	580.2573	Alkaloid	$C_{35}H_{36}N_2O_6$	Daphnoline	0.75	2,287,858
19	34.941	611.3672	611.3682	Alkaloid	$C_{33}H_{49}N_5O_6$	Zizyphine A	−1.71	24,935,381
20	35.517	492.2741	492.2737	Alkaloid	$C_{28}H_{36}N_4O_4$	Mucronine B	0.89	23,735,070
21	38.691	506.3598	506.3607	Triterpenoid	$C_{30}H_{50}O_6$	Theasapogenol A	−1.76	1,480,313
22	38.797	483.3458	483.3468	Alkaloid	$C_{31}H_{46}O_4$	Adlupone	−2.03	2,573,248
23	39.111	276.2102	276.2089	Steroid	$C_{18}H_{28}O_2$	19-Nor-5-androstenediol	4.61	7,083,027
24	40.454	664.3975	664.3975	Phenolic	$C_{40}H_{56}O_8$	3-*O*-trans-Feruloyleuscaphic acid	−0.07	3,481,171
25	41.205	386.2289	386.2305	Sesquiterpenoid	$C_{20}H_{34}O_7$	Oleandolide	−4.11	3,312,096
26	42.077	596.2998	596.2985	Triterpenoid	$C_{34}H_{44}O_9$	Salannin	2.19	10,826,760
27	43.298	554.2529	554.2516	Flavonoid	$C_{31}H_{38}O_9$	Toonacilin	2.32	966680

(Continues)

TABLE 1 | (Continued)

No.	RT	Exp. mass *m/z*	Calc. mass *m/z*	Type	Formula	Tentatively identified compounds	Diff (ppm)	Peak area
28	43.994	582.2703	582.273	Alkaloid	$C_{35}H_{38}N_2O_6$	2′-Norberbamunine	−4.56	2,247,738
29	44.328	646.5674	646.5688	Steroid	$C_{45}H_{74}O_2$	Sitosteryl ester	−2.24	169,347,603
30	46.296	674.3644	674.3666	Glycoside	$C_{37}H_{54}O_{11}$	Cimicifugoside	−3.28	6,121,585
31	46.84	650.6567	650.6577	Fatty acid	$C_{43}H_{86}O_3$	Hydroxyphthioceranic acid (C43)	−1.6	6,830,602
32	47.918	280.2408	280.2402	Fatty acid	$C_{18}H_{32}O_2$	Linoleic acid	2.2	143,255,844
33	49.108	650.3295	650.3302	Sesquiterpene	$C_{34}H_{50}O_{12}$	Thapsigargin	−1.06	9,980,761
34	49.719	466.3809	466.3811	Steroid	$C_{32}H_{50}O_2$	Ergosterol acetate	−0.33	1,526,534
35	51.04	652.2893	652.2897	Alkaloid	$C_{37}H_{40}N_4O_7$	Haplophytine	−0.55	7,917,252
36	51.354	394.1785	394.178	Xanthone	$C_{24}H_{26}O_5$	1,3,8-Trihydroxy-4-methyl-2,7-diprenylxanthone	1.11	2,044,981
37	51.533	394.3604	394.3599	Triterpenoid	$C_{29}H_{46}$	24-Norursa-3,12-diene	1.18	17,385,207
38	52.336	644.5526	644.5532	Steroid	$C_{45}H_{72}O_2$	Stigmasteryl ester	−0.98	813728
39	54.272	396.3759	396.3756	Steroid	$C_{29}H_{48}$	Stigmastan-3,5-diene	0.64	14,154,499
40	57.221	408.3394	408.3392	Steroid	$C_{29}H_{44}O$	Conicasterol B	0.4	15,538,738
41	57.884	586.4957	586.4961	Coumaric	$C_{38}H_{66}O4$	Erythrinasinate A	−0.69	2,747,883
42	59.332	398.3559	398.3549	Steroid	$C_{28}H_{46}O$	Stellasterol	2.53	208,511,860

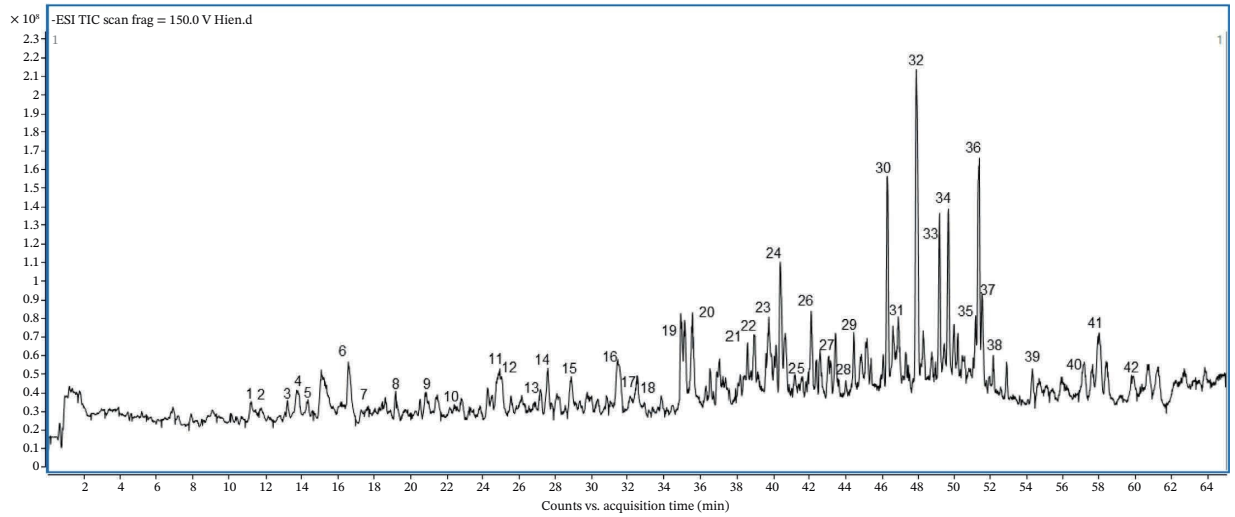


FIGURE 3 | Chromatogram of the EtOH leaf extract of *L. decumana* in negative ion mode obtained by UPLC-QTOF-MS.

biocellulose alone (5.13 ± 0.77 mm) or left untreated (5.06 ± 0.76 mm). However, these differences were not statistically significant. By Day 11, extract-treated wounds appeared visually drier and showed a significantly smaller wound diameter (3.00 ± 0.61 mm) than untreated wounds (4.44 ± 0.73 mm; Tukey's HSD, $p = 0.024$) and wounds treated with biocellulose alone (4.58 ± 0.51 mm; Tukey's HSD, $p = 0.014$).

Wound-healing rates are summarized in Table 2. Overall group differences in percentage wound closure were significant on days 11 and 13 (one-way ANOVA, $p = 0.010$ and $p = 0.009$, respectively). Post hoc analysis confirmed that wounds treated with biocellulose plus LDE achieved significantly greater healing compared with untreated wounds, reaching $50.00 \pm 0.61\%$ closure by Day 11 (Tukey's HSD, $p = 0.024$) and $67.71 \pm 0.43\%$ by Day 13 (Tukey's HSD, $p = 0.026$). Notably, complete wound closure was observed in one rat from this treatment group by Day 15. In contrast, untreated wounds and wounds treated with blank biocellulose showed lower healing percentages by Day 13 ($36.15 \pm 1.10\%$ and $30.38 \pm 0.82\%$, respectively), with complete wound closure occurring only by Day 19.

3.4 | Effect of *L. decumana* Biocellulose Dressing on Wound-Histopathological Changes

Histopathological examination using HE staining in Figure 5 revealed severe inflammation in all wounds by Day 3, characterized by a substantial presence of inflammatory cells, particularly neutrophils, along with a few macrophages. By Day 7, the inflammatory response was still evident, though slightly reduced, especially in untreated wounds and wounds treated with blank biocellulose. Wounds treated with biocellulose containing LDE, however, showed a significant reduction in inflammation. At this stage, signs of proliferation were observed, with fibroblasts beginning to populate the wound surface. A thin collagen layer had also begun to form. Nevertheless, by Day 11, untreated wounds still exhibited some inflammatory response, though its intensity had diminished. The proliferative phase was beginning, although re-epithelialization was not yet pronounced. In wounds treated with blank biocellulose, the number of inflammatory cells had decreased, and both proliferation and re-epithelialization were underway. In contrast, wounds treated with biocellulose plus LDE showed the most advanced maturation and re-epithelialization, with a thicker collagen layer, and epithelial tissue started to develop.

Masson's trichrome staining revealed limited granulation tissue in untreated wounds, even after 11 days postinduction (Figure 6). In wounds treated with blank biocellulose, collagen deposition was prominent; however, re-epithelialization was absent due to ongoing inflammation. Conversely, wounds treated with *L. decumana*–fortified biocellulose displayed established re-epithelialization, although the collagen layer remained comparatively thin.

4 | Discussion

Plant-based therapies are increasingly recognized for their therapeutic potential in wound care. Known to produce a distinct itching sensation when applied to the skin, *L. decumana* has been used empirically for centuries as a pain reliever for conditions such as muscle aches and wound-related discomfort. Toxicological assessments of *L. decumana* have also demonstrated its safety in oral administration at a certain dose [16], supporting its potential for broader medicinal use. In this study, the wound-healing efficacy of *L. decumana* in biocellulose dressings was evaluated in polymicrobial-infected wounds.

4.1 | *L. decumana* Effects on Wound-Healing Process

This study demonstrates that LDE incorporated into a biocellulose dressing significantly enhances wound healing in a polymicrobial-infected rat model. Although no marked differences were evident during the early inflammatory period (Day 3), wounds treated with *L. decumana* showed accelerated wound contraction from Day 11 onward, accompanied by reduced exudate and earlier wound drying. These findings are consistent with previous reports, demonstrating that topical application of *L. decumana* significantly promotes acute wound healing, particularly during the proliferative and maturation phases [14].

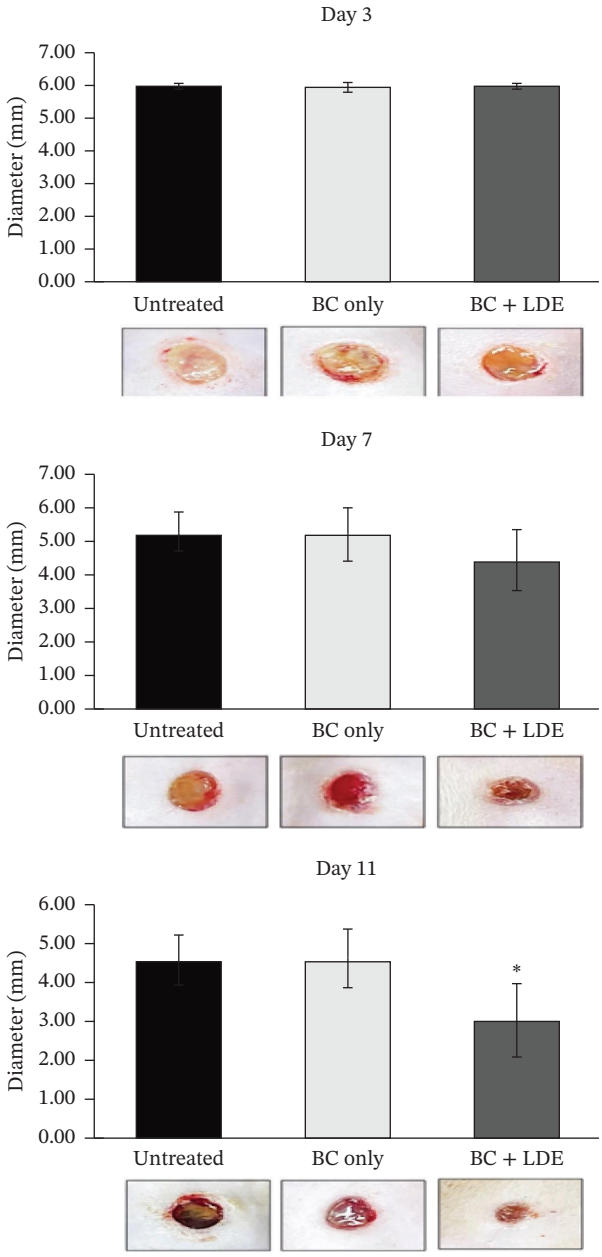


FIGURE 4 | Wound diameter (mm) of untreated wounds and wounds treated with biocellulose (BC) with or without *Laportea decumana* extract (LDE) on Days 3, 7, and 11. Data are presented as mean ± SD ($n = 5$ per group). Statistical analysis was performed using one-way ANOVA followed by Tukey's HSD post hoc test. $^{*}p < 0.05$ compared with untreated and BC-only groups. Representative wound images are shown.

During the proliferative phase (Day 7), untreated wounds and those treated with blank biocellulose displayed persistent inflammatory cell infiltration, indicating delayed resolution of inflammation. This prolonged inflammatory response is likely attributable to the polymicrobial infection, as inflammation in normal wound healing typically resolves within 2–5 days [17]. Polymicrobial wounds are frequently complicated by biofilm formation, in which microorganisms embedded within a protective extracellular polymeric matrix evade host immune defenses and antimicrobial agents, thereby prolonging inflammation [18]. In contrast, wounds treated with LDE showed a marked reduction in inflammatory cells, suggesting more efficient inflammatory resolution. While inflammatory mediators were not directly quantified in this study, prior reports indicate that crude ethanolic extracts of *L. decumana* exhibit COX-2 inhibitory activity, suppression of IL-6, and moderate free radical scavenging capacity [9, 19, 20], which may contribute to the observed histological improvements. In addition, the antibacterial activities of *Laportea* extract reported in other studies [21, 22] may support microbial control in infected wounds and potentially facilitate the resolution of the inflammatory phase.

The wound-healing efficacy observed in this study likely arises from the combined actions of multiple phytochemicals present in *L. decumana*. Botanical extracts rich in polyphenols, flavonoids, and triterpenoids are known to promote wound repair through coordinated antioxidant, anti-inflammatory, and antimicrobial mechanisms, with therapeutic effects often attributed to synergistic interactions rather than a single active compound [23, 24]. Furthermore, the use of biocellulose as a delivery matrix may have enhanced these effects by improving local retention and bioavailability of the extract while providing a moist, protective environment [23].

4.2 | Phytochemical Constituents of *L. decumana* and Their Potential Contribution

The UPLC-Q-TOF/MS analysis revealed several bioactive compounds with antimicrobial, antioxidant, and anti-inflammatory properties, supporting the potential use of the EtOH extract as a wound-healing agent.

Antimicrobial activity. A range of compounds with antimicrobial properties was detected in the EtOH extract of *L. decumana* leaf. Palmatine **(10)**, integerrenine **(14)**, and mucronine B **(20)** have been reported to exert antibacterial effects [25–27]. Sitosteryl ester **(29)** and stellasterol **(42)** have also been linked to antibacterial activity [28, 29], while stigmasteryl ester **(38)** exhibits both antibacterial and antifungal properties [30, 31]. Additionally, flavonoids such as capparilloside A **(8)** and toonacilin **(27)** possess antimicrobial effects [32, 33], while salannin **(26)** shows broad-spectrum antimicrobial activity [34]. Furthermore, carboxylic and cinnamic acids, including 3-(2,5-dimethoxyphenyl)propanoic acid **(3)** and 4-methoxycinnamic acid **(5)**, also contribute to antimicrobial effects [35, 36].

Anti-inflammatory activity. Several compounds identified in the extract demonstrate anti-inflammatory potential, which is essential for modulating the wound-healing process. Alkaloid palmatine **(10)** and 2′-norberbamunine **(28)** have demonstrated anti-inflammatory properties, with the latter known for suppressing nitric oxide, a key inflammatory mediator [25, 37]. In addition to anti-inflammatory effects, artesunate **(9)** and 11α-acetoxykhivorin **(15)** also exhibit antiparasitic and anticancer properties [38–41]. Meanwhile, steroid stigmastan-3,5-diene **(39)** and stellasterol **(42)** [29, 42], as well as flavonoids capparilloside A **(8)** and toonacilin **(27)**, may further enhance the extract's anti-inflammatory potential [32, 33].

Antioxidant activity. Oxidative stress plays a critical role in delaying wound healing, making antioxidants valuable in the treatment process. Several compounds were identified with antioxidant activity. Salannin **(26)** and stigmasteryl ester **(38)**

TABLE 2 | The rates of wound healing with different treatments.

Treatments	Percentage of healing (%)						
	Day 1	Day 3	Day 5	Day 7	Day 9	Day 11	Day 13
Untreated	0.0 ± 0.00	0.56 ± 0.09	11.67 ± 0.64	15.63 ± 0.76	22.92 ± 0.71	26.04 ± 0.73	36.15 ± 1.10
BC only	0.0 ± 0.00	1.11 ± 0.15	12.08 ± 0.75	14.58 ± 0.77	17.08 ± 0.77	23.61 ± 0.51	30.38 ± 0.82
BC + LDE	0.0 ± 0.00	0.56 ± 0.09	17.22 ± 0.74	26.46 ± 0.82	38.33 ± 0.93	50.00 ± 0.61*	67.71 ± 0.43*
p value	1.00[a]	0.809[a]	0.361[a]	0.099[b]	0.072[b]	0.010[b]	0.009[b]

Note: Data are presented as mean ± SD ($n = 5$ per group). *p* values indicate overall group differences at each time point determined by [a]Kruskal–Wallis test or [b]one-way ANOVA. When overall differences were significant, pairwise comparisons were performed using Tukey's HSD post hoc test.
*$p < 0.05$ for BC + LDE compared with untreated wounds and BC only treatment in post hoc analysis.

have demonstrated antioxidant potential [31, 34]. Ergosterol acetate **(34)** has been shown to reduce the levels of radical oxygen species, thereby reducing cell damage [43, 44]. Another compound, 24-norursa-3,12-diene **(37)**, has also been found as the major component in *Ochradenus arabicus* essential oil. This compound was believed to contribute to the plant's potent antioxidant activity [45].

Wound-healing potential. Beyond antimicrobial, anti-inflammatory, and antioxidant effects, some compounds have been directly linked to wound healing. Corchoionoside B (**2**) enhances fibroblast proliferation, a key factor in tissue regeneration [46]. Conicasterol B (40) has been shown to provide cellular protection, which may contribute to tissue repair [46]. Rebaudioside B (**1**) has been reported to reduce inflammation and apoptosis in lung ischemia–reperfusion injury [47]. Haplophytine (**35**) activates protein kinase C alpha (PRKCA), a key enzyme involved in regulating cell growth, migration, and angiogenesis, thereby promoting faster wound closure and improved healing [48]. Artesunate (**9**) reduces hypertrophic scar formation by inhibiting excessive collagen and fibroblast proliferation, thereby enhancing wound healing [49].

The presence of multiple bioactive compounds with antimicrobial, anti-inflammatory, and antioxidant properties supports the therapeutic potential of LDE as a wound-healing agent. Consistent with this, our previous study demonstrated that topical application *of L. decumana* ethanolic extract

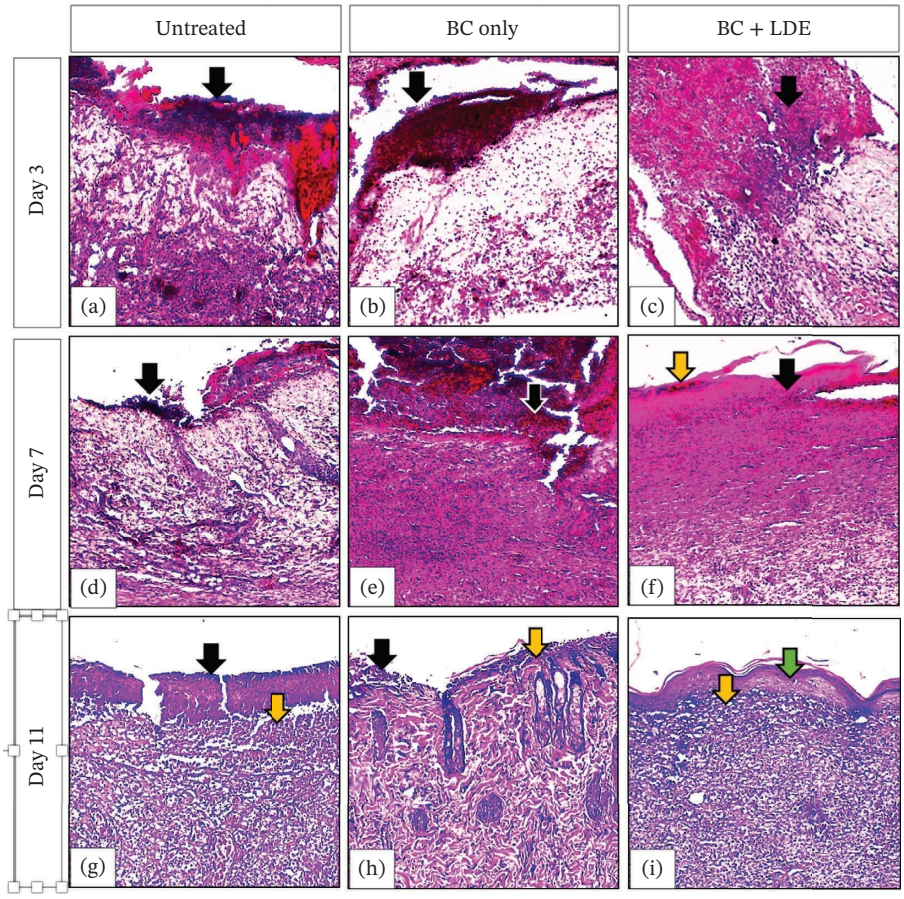


FIGURE 5 | Microscopic photograph of wounds with different treatments on Days 3, 7, and 11 using hematoxylin and eosin staining. Black arrows represent inflammatory cell infiltration; yellow arrows represent proliferation of fibroblast; green arrow represents re-epithelization. Pictures were taken with 10x and 40x magnification.

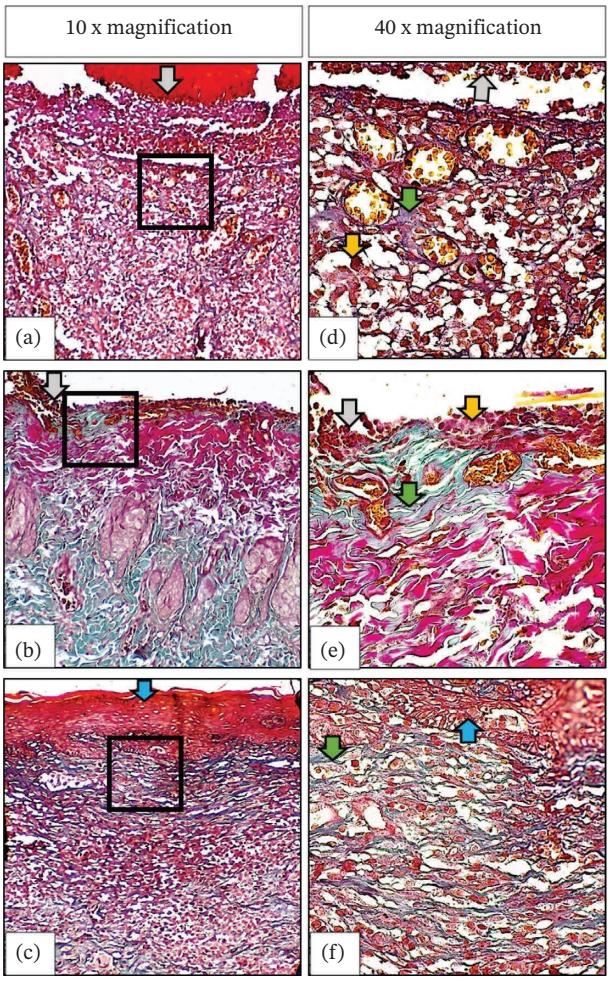


FIGURE 6 | Microscopic photograph of wounds left untreated (a, d), treated with BC only (b, e), and treated with BC + LDE (c, f) after Day 11 using Masson's trichrome staining. Grey arrows represent inflammatory cell infiltration; yellow arrows represent granulation tissue; green arrows represent collagen deposition; blue arrows represent re-epithelization. Pictures were taken with 10x and 40 x magnification.

significantly reduced IL-6, a key proinflammatory cytokine involved in inflammation [9]. Moreover, the extract has been shown to enhance fibroblast activity, supporting collagen synthesis and tissue remodeling in acute wounds [14]. The present study further demonstrates its efficacy in infected wounds, suggesting a dual role in infection control and tissue repair. While these findings are limited to a preclinical model, practical considerations such as sterilization compatibility and formulation stability warrant further evaluation prior to clinical translation.

4.3 | Limitations of the Study

This study has several limitations that should be acknowledged. First, although UPLC-QTOF/MS enabled high-confidence, putative identification of bioactive compounds in LDE, compound annotation was based on accurate mass, isotopic pattern, and database matching without confirmation using authentic reference standards or NMR analysis. Therefore, the identified compounds should be considered tentative and warrant further validation. Second, while biocellulose was prepared using a validated and standardized protocol, detailed physicochemical characterization of the dressing, including thickness, porosity, and water retention capacity, was not quantitatively assessed. These parameters may influence dressing performance and should be systematically evaluated in future studies. Third, no *in vitro* antibacterial or anti-inflammatory assays were performed to directly validate the antimicrobial or immunomodulatory activities of the LDE or the biocellulose-based formulation; thus, the observed wound-healing effects are based on healing outcomes and warrant further mechanistic investigation. Fourth, a formal dose–response analysis was not performed, as only a single extract concentration was incorporated into the biocellulose dressing. Consequently, the optimal therapeutic dose and concentration–effect relationship remain to be determined. Finally, while the within-animal design minimized interanimal variability and animal use, potential local or systemic cross-influences between wounds may represent a methodological limitation that should be considered when interpreting the results.

5 | Conclusion

In conclusion, the 4% LDE-fortified biocellulose dressing improved wound-healing outcomes in the polymicrobial-infected rat model, with statistically significant enhancement observed at later stages of healing. Histopathological and morphological findings suggest that LDE may support tissue repair by promoting fibroblast infiltration and accelerating re-epithelialization. UPLC-Q-TOF/MS analysis tentatively identified 42 compounds, predominantly alkaloids, steroids, triterpenoids, sesquiterpenes, and flavonoids, several of which are reported to possess anti-inflammatory, antimicrobial, and antioxidant properties.

These findings suggest that *L. decumana*–loaded biocellulose dressings may serve as a bioactive approach to support healing in infected wounds. Nevertheless, further studies are required to elucidate the underlying mechanisms, optimize dosing, and evaluate safety and efficacy across different wound models to better define their translational potential.

Author Contributions

Yulia Yusrini Djabir: funding acquisition, resources, conceptualization, supervision, formal analysis, writing–original draft. Dwi Novrianty Busaeri: investigation, data curation, visualization, formal analysis. Muhammad Haryandi: investigation, data curation. Nurhasni Hasan: conceptualization, methodology. Habibie Habibie: writing–review and editing. Djulfikri Mewar: investigation, methodology. Hien Minh Nguyen: investigation, writing–review and editing. Aryadi Arsyad: investigation, methodology, writing–review and editing.

Acknowledgments

The authors would like to thank Abdul Rahim, PhD, for his invaluable assistance in the identification of *Laportea decumana*. The authors would also like to acknowledge the support and collaborative contribution of the Faculty of Pharmacy, Ton Duc Thang University, Vietnam.

Funding

This study was financially supported by the Hasanuddin University Internal Funding under the Fundamental Collaboration Research Grant Scheme (Contract No. 00309/UN4.22/PT/01/03/2024).

Ethics Statement

All animal-related experimental procedures strictly adhered to the institutional guidelines for the ethical care and use of laboratory animals. The ethical approval was granted by the Research Ethics Committee of the Medical Faculty, Hasanuddin University (No. 498/UN4.6.4.5.3L/PP36/2023), valid until July 2024.

Conflicts of Interest

The authors declare no conflicts of interest.

Data Availability Statement

The data that support the findings of this study are available from the corresponding author upon reasonable request.

References

1. S. Bertesteanu, S. Triaridis, M. Stankovic, et al., "Polymicrobial Wound Infections: Pathophysiology and Current Therapeutic Approaches," *International Journal of Pharmacy* 463, no. 2 (2014): 119–126, https://doi.org/10.1016/j.ijpharm.2013.12.012.

2. M. Rodrigues, N. Kosaric, C. A. Bonham, and G. C. Gurtner, "Wound Healing: A Cellular Perspective," *Physiological Reviews* 99, no. 1 (2019): 665–706, https://doi.org/10.1152/physrev.00067.2017.

3. H. Sorg, D. J. Tilkorn, S. Hager, J. Hauser, and U. Mirastschijski, "Skin Wound Healing: An Update on the Current Knowledge and Concepts," *European Surgical Research* 58, no. 1-2 (2017): 81–94, https://doi.org/10.1159/000454919.

4. M. Horue, J. M. Silva, I. R. Berti, L. R. Brandão, H. D. S. Barud, and G. R. Castro, "Bacterial Cellulose-Based Materials as Dressings for Wound Healing," *Pharmaceutics* 15, no. 2 (2023): 424, https://doi.org/10.3390/pharmaceutics15020424.

5. W. He, J. Wu, J. Xu, D. A. Mosselhy, Y. Zheng, and S. Yang, "Bacterial Cellulose: Functional Modification and Wound Healing Applications," *Advances in Wound Care* 10, no. 11 (2021): 623–640, https://doi.org/10.1089/wound.2020.1219.

6. P. Shrivastav, S. Pramanik, G. Vaidya, et al., "Bacterial Cellulose as a Potential Biopolymer in Biomedical Applications: A State-of-the-Art Review," *Journal of Materials Chemistry B* 10, no. 17 (2022): 3199–3241, https://doi.org/10.1039/d1tb02709c.

7. R. Rollando, E. Monica, M. Afthoni, C. Kurniawan, and R. Sitepu, "Isolation and Evaluation of Pharmacological Activities of a Bioactive Hydroxylated C28 Steroid From the Leaf of *Laportea decumana* (Roxb.) Wedd," *Tropical Journal of Natural Product Research* 6 (2022): 1096–1102.

8. B. Lukman La, S. Djoko, M. Retno, and H. Triana, "Uncover Itchy Leaves Ethnomedicine Usage: A Preliminary Study on Characterization and Bioactivity of Laportea Spp," *Pharmaceutical Journal* 14, no. 4 (2022): 286–295.

9. D. Mewar, Y. Djabir, and G. Alam, "Topical Anti-Inflammatory and Analgesic Activities of Laportea decumana (Roxb) Wedd Extract Cream in Rats," *Journal of Research in Pharmacy* 27, no. 5 (2023): 2026–2034, https://doi.org/10.29228/jrp.482.

10. P. S. S. Sofini, D. J. Mercy, V. Raghavan, et al., "Evaluation of Scarless Wound Healing Through Nanohydrogel Infused With Selected Plant Extracts," *Journal of Drug Delivery Science and Technology* 100 (2024): 106118, https://doi.org/10.1016/j.jddst.2024.106118.

11. J. D. Mercy, A. Thirumalai, S. Udayakumar, et al., "Enhancing Wound Healing With Nanohydrogel-Entrapped Plant Extracts and Nanosilver: An In Vitro Investigation," *Molecules* 29, no. 21 (2024).

12. N. Jangra, A. Singla, V. Puri, et al., "Herbal Bioactive-Loaded Biopolymeric Formulations for Wound Healing Applications," *RSC Advances* 15, no. 16 (2025): 12402–12442, https://doi.org/10.1039/d4ra08604j.

13. N. Hasan, J. Lee, H. J. Ahn, et al., "Nitric Oxide-Releasing Bacterial Cellulose/Chitosan Crosslinked Hydrogels for the Treatment of Polymicrobial Wound Infections," *Pharmaceutics* 14, no. 1 (2021): 22, https://doi.org/10.3390/pharmaceutics14010022.

14. D. N. Busaeri, Y. Y. Djabir, R. Agustina, G. Alam, D. Mewar, and S. Nadiah, "The Effect of the Ethanolic Extract of Laportea decumana (Roxb.) Wedd. on the Inflammatory, Proliferative and Maturation Stages of Wound Healing of an Acute Injury Using a Rat Model," *Journal of Research in Pharmacy* 29, no. 1 (2025): 81–90, https://doi.org/10.12991/jrespharm.1626448.

15. J. L. Brown, E. Townsend, R. D. Short, et al., "Assessing the Inflammatory Response to In Vitro Polymicrobial Wound Biofilms in a Skin Epidermis Model," *NPJ Biofilms Microbiomes* 8, no. 1 (2022): 19, https://doi.org/10.1038/s41522-022-00286-z.

16. Y. G. Hasan, Y. Y. Djabir, G. Alam, et al., "Acute and Subacute Toxicity Study of Laportea decumana Leaf Extract in Rats," *Farmacia* 72, no. 3 (2024): 645–654, https://doi.org/10.31925/farmacia.2024.3.19.

17. S. K. Shukla, A. K. Sharma, V. Gupta, and M. H. Yashavarddhan, "Pharmacological Control of Inflammation in Wound Healing," *Journal of Tissue Viability* 28, no. 4 (2019): 218–222, https://doi.org/10.1016/j.jtv.2019.09.002.

18. Y. Almuhanna, "Microbial Biofilms as Barriers to Chronic Wound Healing: Diagnostic Challenges and Therapeutic Advances," *Journal of Clinical Medicine* 14, no. 22 (2025): 8121, https://doi.org/10.3390/jcm14228121.

19. L. La Basy, T. Hertiani, R. Murwanti, and E. Damayanti, "Investigation of Cox-2 Inhibition of Laportea decumana (Roxb). Wedd Extract to Support Its Analgesic Potential," *Journal of Ethnopharmacology* 318 (2024): 116857, https://doi.org/10.1016/j.jep.2023.116857.

20. E. S. Simaremare, M. R. Y. Tolip, and R. D. Pratiwi, "Formulation and Effectiveness Test of Analgesic Patch From Itchy Leaves (Laportea decumana (Roxb.) Wedd)," *Current Journal of Applied Science and Technology* 22, no. 3 (2022): 1–13.

21. W. D. Gunardi, S. E. Sudradjat, and K. H. Timotius, "Healing Capacities of Nettles: Dendrocnide, Girardinia, Laportea, and Urtica," *Phytomedicine Plus* 3, no. 2 (2023): 100438, https://doi.org/10.1016/j.phyplu.2023.100438.

22. E. Simaremare, E. Gunawan, I. Yarangga, M. Satya, and Y. Yabansabra, "Antibacterial and Toxicity Activities Itchy Leaves (*Laportea decumana*, Roxb. Wedd) Extract," *Journal of Physics. Conference Series* 1503, no. 1 (2020): 012041, https://doi.org/10.1088/1742-6596/1503/1/012041.

23. S. El-Sherbeni and W. Negm, "The Wound Healing Effect of Botanicals and Pure Natural Substances Used in In Vivo Models," *Inflammopharmacology* 31, no. 2 (2023): 755–772, https://doi.org/10.1007/s10787-023-01157-5.

24. S. Vitale, S. Colanero, M. Placidi, et al., "Phytochemistry and Biological Activity of Medicinal Plants in Wound Healing: An Overview of Current Research," *Molecules* 27, no. 11 (2022): 3566, https://doi.org/10.3390/molecules27113566.

25. J. Long, J. Song, L. Zhong, Y. Liao, L. Liu, and X. Li, "Palmatine: A Review of Its Pharmacology, Toxicity and Pharmacokinetics," *Biochimie* 162 (2019): 176–184, https://doi.org/10.1016/j.biochi.2019.04.008.

26. H. R. El-Seedi, S. Gohil, P. Perera, K. B. G. Torssell, and L. Bohlin, "Cyclopeptide Alkaloids from Heisteria nitida," *Phytochemistry* 52, no. 8 (1999): 1739–1744, https://doi.org/10.1016/s0031-9422(99)00183-1.

27. N. I. Mongalo, S. S. Mashele, and T. J. Makhafola, "Ziziphus mucronata Willd. (Rhamnaceae): It's Botany, Toxicity, Phytochemistry and Pharmacological Activities," *Heliyon* 6, no. 4 (2020): e03708, https://doi.org/10.1016/j.heliyon.2020.e03708.

28. I. A. Evangelina, Y. Herdiyati, A. Laviana, R. Rikmasari, C. Zubaedah, and K. D. Anisah, "Bio-Mechanism Inhibitory Prediction of

β-Sitosterol From Kemangi (*Ocimum basilicum* L.) as an Inhibitor of MurA Enzyme of Oral Bacteria: In Vitro and In Silico Study," *Advances and Applications in Bioinformatics and Chemistry* 14 (2021): 103–115, https://doi.org/10.2147/aabc.s301488.

29. Y. R. Consolacion, S. T. Maria Carmen, C. Ellenita De, M. D. L. R. Mariquit, G. O. Glenn, and S. Chien-Chang, "Sterols From Lentinus tigrinus," *Pharmacognosy Journal* 10, no. 6 (2018): 1079–1081.

30. Y. A. Kim and H. K. Kim, "Antibacterial Activity of a Linolenic Acid Stigmasterol Ester Produced by Lipase-Mediated Transesterification," *Journal of Microbiology and Biotechnology* 35 (2025): e2410055, https://doi.org/10.4014/jmb.2410.10055.

31. M. Goswami, J. S. Priya, G. D. Gupta, and S. K. Verma, "A Comprehensive Update on Phytochemistry, Analytical Aspects, Medicinal Attributes, Specifications and Stability of Stigmasterol," *Steroids* 196 (2023): 109244, https://doi.org/10.1016/j.steroids.2023.109244.

32. H. Gou, J. Ye, Y. Wang, et al., "The Anti-Inflammatory Activity of Toonaciliatin K Against Adjuvant Arthritis," *BioMed Research International* 2017 (2017): 9436280–12, https://doi.org/10.1155/2017/9436280.

33. Z. Li, J. Zhao, H. Zhou, et al., "Capparilоside A Shows Antiviral and Better Anti-inflammatory Effects Against Influenza Virus via Regulating Host IFN Signaling, In Vitro and Vivo," *Life Sciences* 200 (2018): 115–125, https://doi.org/10.1016/j.lfs.2018.03.033.

34. A. VasudhaUdupa, B. Gowda, B. E. Kumarswammy, and M. B. Shivanna, "The Antimicrobial and Antioxidant Property, GC–MS Analysis of Non-Edible Oil-Seed Cakes of Neem, Madhuca, and Simarouba," *Bulletin of the National Research Centre* 45, no. 1 (2021): 41, https://doi.org/10.1186/s42269-021-00498-x.

35. Y. Wang, M. Yin, L. Gu, et al., "The Therapeutic Role and Mechanism of 4-Methoxycinnamic Acid in Fungal Keratitis," *International Immunopharmacology* 116 (2023): 109782, https://doi.org/10.1016/j.intimp.2023.109782.

36. J.-W. Jeong, I.-W. Choi, G.-H. Jo, et al., "Anti-Inflammatory Effects of 3-(4′-Hydroxyl-3′,5′-Dimethoxyphenyl)Propionic Acid, an Active Component of Korean Cabbage Kimchi, in Lipopolysaccharide-Stimulated BV2 Microglia," *Journal of Medicinal Food* 18, no. 6 (2015): 677–684, https://doi.org/10.1089/jmf.2014.3275.

37. D. N. Tu, V. T. B. Hau, N. T. Diep, et al., "Alkaloids from Phaeanthus Vietnamensis With Inhibitory Effect on Nitric Oxide Production lipopolysaccharide-stimulated in RAW264.7 Macrophages," *Journal of Asian Natural Products Research* 24, no. 9 (2022): 898–903, https://doi.org/10.1080/10286020.2021.1993833.

38. A. S. Miranda, F. Brant, N. P. Rocha, et al., "Further Evidence for an Anti-Inflammatory Role of Artesunate in Experimental Cerebral Malaria," *Malaria Journal* 12, no. 1 (2013): 388, https://doi.org/10.1186/1475-2875-12-388.

39. S. Zuo, Q. Li, X. Liu, H. Feng, and Y. Chen, "The Potential Therapeutic Effects of Artesunate on Stroke and Other Central Nervous System Diseases," *BioMed Research International* 2016, no. 1 (2016): 1489050–16, https://doi.org/10.1155/2016/1489050.

40. K. S. Ravikumar, H. Ramya, T. A. Ajith, M. A. Shah, and K. K. Janardhanan, "Bioactive Extract of Fomitopsis Pinicola Rich in 11-*α*-Acetoxykhivorin Mediates Anticancer Activity by Cytotoxicity, Induction of Apoptosis, Inhibition of Tumor Growth, Angiogenesis and Cell Cycle Progression," *Journal of Functional Foods* 78 (2021): 104372, https://doi.org/10.1016/j.jff.2021.104372.

41. K. Yoshikawa, M. Inoue, Y. Matsumoto, et al., "Lanostane Triterpenoids and Triterpene Glycosides From the Fruit Body of Fomitopsis pinicola and Their Inhibitory Activity Against COX-1 and COX-2," *Journal of Natural Products* 68, no. 1 (2005): 69–73, https://doi.org/10.1021/np040130b.

42. S. Park, Y.-W. Kim, M. Park, S. Byun, S. Kim, and J. Lee, "Anti-Inflammatory Steroid From Phragmitis Rhizoma Modulates LPS-Mediated Signaling Through Inhibition of NF-κB Pathway," *Inflammation* 39, no. 2 (2016): 727–734, https://doi.org/10.1007/s10753-015-0299-6.

43. P. Rangsinth, R. Sharika, N. Pattarachotanant, et al., "Potential Beneficial Effects and Pharmacological Properties of Ergosterol, a Common Bioactive Compound in Edible Mushrooms," *Foods* 12, no. 13 (2023): 2529, https://doi.org/10.3390/foods12132529.

44. Z. Yongxia, X. Jian, H. Suyuan, N. Aixin, and Z. Lihong, "ISOLATION and Characterization of Ergosterol From Monascus Anka for Anti-lipid Peroxidation Properties," *Journal de Mycologie Medicale* 30, no. 4 (2020): 101038, https://doi.org/10.1016/j.mycmed.2020.101038.

45. O. Ullah, M. Shah, N. U. Rehman, et al., "Aroma Profile and Biological Effects of Ochradenus arabicus Essential Oils: A Comparative Study of Stem, Flowers, and Leaves," *Molecules* 27, no. 16 (2022): 5197, https://doi.org/10.3390/molecules27165197.

46. N. H. Shady, A. H. Altemani, F. H. Altemani, et al., "The Potential of Corchorus Olitorius Seeds Buccal Films for Treatment of Recurrent Minor Aphthous Ulcerations in Human Volunteers," *Molecules* 27, no. 20 (2022): 7020, https://doi.org/10.3390/molecules27207020.

47. X. Wu, T. Qiao, J. Huang, et al., "Rebaudioside B Attenuates Lung Ischemia-Reperfusion Injury Associated Apoptosis and Inflammation," *Recent Adv Inflamm Allergy Drug Discov* 18, no. 2 (2024): 156–166, https://doi.org/10.2174/0127722708295154240327035857.

48. N. R. Chanu, K. Bhattacharya, and S. Sen, "From Nature to Healing: How *Gynura cusimbua* May Support Diabetic Wound Recovery," *Food Bioscience* 68 (2025): 106544, https://doi.org/10.1016/j.fbio.2025.106544.

49. J. Zhang, S. Zhou, Z. Xia, et al., "Effectiveness of Artesunate Combined With Fractional CO2 Laser in a Hypertrophic Scar Model With Underlying Mechanism," *Burns* 48, no. 3 (2022): 662–671, https://doi.org/10.1016/j.burns.2021.05.013.